Spin-orbit-induced orbital excitations in Sr_2RuO_4 and Ca_2RuO_4: A resonant inelastic x-ray scattering study

C. G. Fatuzzo,[1] M. Dantz,[2] S. Fatale,[1] P. Olalde-Velasco,[2] N. E. Shaik,[1] B. Dalla Piazza,[1] S. Toth,[3] J. Pelliciari,[2] R. Fittipaldi,[4,5] A. Vecchione,[4,5] N. Kikugawa,[6,7] J. S. Brooks,[7] H. M. Rønnow,[1,8] M. Grioni,[1] Ch. Rüegg,[3,9] T. Schmitt,[2] and J. Chang[1,10]

[1]*Institute for Condensed Matter Physics, École Polytechnique Fedérale de Lausanne (EPFL), CH-1015 Lausanne, Switzerland*

[2]*Swiss Light Source, Paul Scherrer Institut, CH-5232 Villigen PSI, Switzerland*

[3]*Laboratory for Neutron Scattering and Imaging, Paul Scherrer Institut, CH-5232 Villigen PSI, Switzerland*

[4]*CNR-SPIN, I-84084 Fisciano, Salerno, Italy*

[5]*Dipartimento di Fisica "E.R. Caianiello", Università di Salerno, I-84084 Fisciano, Salerno, Italy*

[6]*National Institute for Materials Science, 1-2-1 Sengen, Tsukuba, 305-0047, Japan*

[7]*National High Magnetic Field Laboratory, Tallahassee, Florida 32310, USA*

[8]*Institute for Solid State Physics (ISSP), The University of Tokyo, Kashiwa, Chiba 277-8581, Japan*

[9]*Department of Quantum Matter Physics, University of Geneva, CH-12111 Geneva, Switzerland*

[10]*Physik-Institut, Universität Zürich, Winterthurerstrasse 190, CH-8057 Zürich, Switzerland*

(Received 19 December 2014; revised manuscript received 2 March 2015; published 6 April 2015)

High-resolution resonant inelastic x-ray scattering (RIXS) at the oxygen K edge has been used to study the orbital excitations of Ca_2RuO_4 and Sr_2RuO_4. In combination with linear dichroism x-ray absorption spectroscopy, the ruthenium $4d$-orbital occupation and excitations were probed through their hybridization with the oxygen p orbitals. These results are described within a minimal model, taking into account crystal field splitting and a spin-orbit coupling $\lambda_{so} = 200$ meV. The effects of spin-orbit interaction on the electronic structure and implications for the Mott and superconducting ground states of $(Ca,Sr)_2RuO_4$ are discussed.

DOI: 10.1103/PhysRevB.91.155104 PACS number(s): 74.70.Pq, 71.70.Ej, 78.70.Dm

I. INTRODUCTION

The relativistic coupling between electronic spin and orbital momentum was long thought to have marginal influence on electrons in solids. Following the prediction and observation of topological surface states on Bi-based compounds [1], this paradigm has changed. The discovery of novel quantum phases realized through strong spin-orbit interaction is now a vivid field of research [2]. The demonstration of spin-orbit coupling driving a new type of Mott insulating state in layered iridates [3] is a good example of this. It has been proposed that doping of this effective $J_{1/2}$-Mott insulating state could lead to an exotic type of superconductivity [4], where Cooper pairs are composed of strongly spin-orbit coupled electrons.

In this context, it is interesting to study other systems that display Mott physics and superconductivity in conjunction with strong spin-orbit interaction. The $4d$ transition-metal oxide system $Ca_{2-x}Sr_xRuO_4$ represents such a case. For $x = 0$, the system is a Mott insulator, whose exact nature is not clarified [5–10]. At the opposite stoichiometric end ($x = 2$), the system has a superconducting ground state ($T_c = 1.5$ K) originating from a correlated Fermi liquid [11]. Although triplet p-wave superconductivity was proposed early on, the mechanism and symmetry class of the superconducting order parameter is still debated [12–16].

A fundamental question is how strongly spin-orbit interaction influences the electrons in these materials and whether it has an impact on the Mott insulating and superconducting ground states. Current experimental evidence for a strong spin-orbit interaction stems from absorption spectroscopy [17–19], which has revealed a considerable admixture of the ruthenium t_{2g} orbitals. More recently, spin-resolved photoemission spectroscopy has reported spin-polarized bands in Sr_2RuO_4 [20,21]. However, the most direct consequence of strong spin-orbit interaction—the splitting of t_{2g} states—has not yet been probed directly by experiments. Orbital excitations transferred across this splitting are in fact not accessible to optical spectroscopies. Furthermore, the Ru L edge (∼3 keV) [9] is currently inaccessible to high-resolution RIXS instrumentation (as it lies right between soft and hard x-ray optics).

To overcome these experimental challenges, we access here the Ru $4d$-orbital excitations through their hybridization with oxygen p orbitals. Exploiting a combination of x-ray absorption (XAS) and oxygen K-edge resonant inelastic x-ray spectroscopy (RIXS), we provide direct evidence for a splitting of the ruthenium t_{2g} states. Our RIXS study of Ca_2RuO_4 and Sr_2RuO_4 reveals excitations that allow an estimation of the spin-orbit coupling, in the same fashion as for the iridates [22,23]. These results suggest a spin-orbit coupling λ_{so} of ∼200 meV—only about two times weaker than in the iridates. We conclude by discussing the Mott insulating and superconducting states in $Ca_{2-x}Sr_xRuO_4$.

II. METHODS

High-quality single crystals of Sr_2RuO_4 and Ca_2RuO_4 were grown by the flux-feeding floating-zone technique [24,25]. The samples were aligned *ex situ* and cleaved *in situ* using the top-post method, to access momenta along the Ru-O bond direction. Oxygen K-edge XAS and RIXS experiments were carried out at the ADvanced RESonant Spectroscopy (ADRESS) beamline at the Swiss Light Source [26,27]. Absorption spectra were measured in fluorescence-yield mode, using both horizontally and vertically polarized light. The RIXS spectrometer was set to have a fixed scattering angle

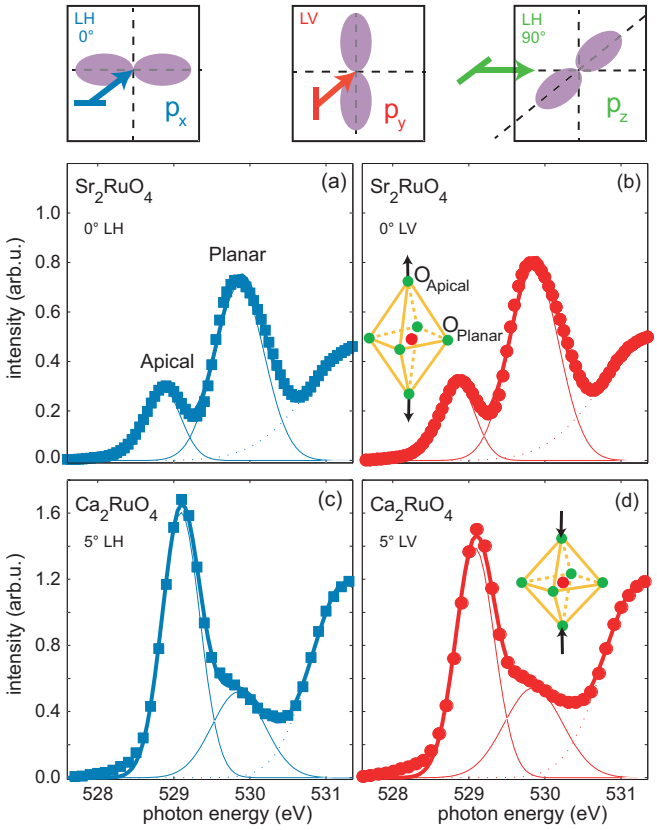

FIG. 1. (Color online) XAS of Sr_2RuO_4 (top) and Ca_2RuO_4 (bottom) recorded using horizontal (left) and vertical (right) linearly polarized light near normal incidence ($\theta \sim 0^\circ$). A sloping background has been subtracted and solid lines are Gaussian fits. Top panels show schematically the oxygen p_x, p_z, and p_y orbitals and how the cross section is optimized with different conditions of incident photon angle and polarization. Lower insets show the elongated and compressed octahedron.

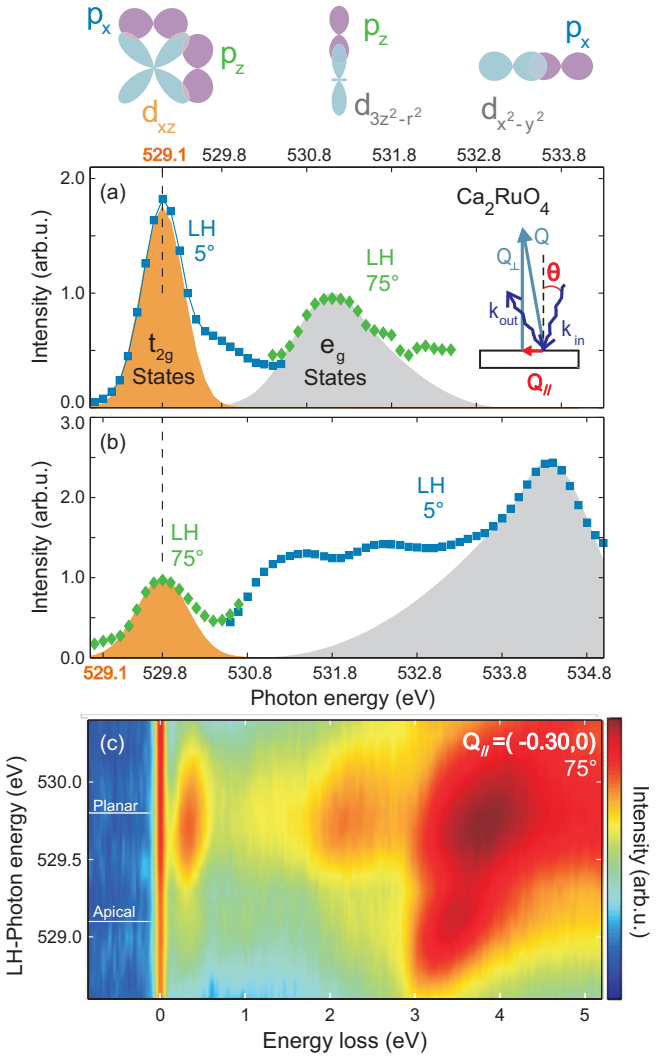

FIG. 2. (Color online) Ca_2RuO_4. (a),(b) X-ray absorption spectra recorded with linear horizontal light and incident angle $\theta = 5^\circ$ (blue squares) and 75° (green diamonds). (a) Absorption spectra mainly probing apical oxygen orbitals, whereas XAS shown in (b) are mostly sensitive to planar oxygen states. Intensities in (a) and (b) are normalized to give approximative overlaps between the two curves. Top panels schematically show the hybridization between Ru d states and oxygen $p_{x/y}$ or p_z orbitals (top). The inset in (a) illustrates the scattering geometry, the incident angle θ, and momentum transfer Q. (c) Resonant inelastic x-ray spectra collected with momentum transfer and polarization as indicated and displayed using a logarithmic color scale as a function of incident photon energy. Notice that the photon energies in (b) are shifted relatively to (a), so that both apical and planar t_{2g} resonances are aligned. Furthermore, the elastic line was aligned to the XAS t_{2g} resonances in (a) and (b), to allow a direct comparison between RIXS and XAS features.

of 130° and an energy resolution of 29 meV (half width at half maximum) at the oxygen K edge. All spectra were recorded at $T = 20$ K. XAS matrix elements and RIXS momentum $Q = (h,k,l)$ were varied by changing the incident angle θ [see inset Fig. 2(a)].

III. RESULTS

In Figs. 1 and 2, x-ray absorption spectra recorded on Ca_2RuO_4 and Sr_2RuO_4 are shown for different light polarizations and incident angles θ. Good agreement with previous XAS work [17,18] is found whenever overlap in temperature, polarization, and incident angle is present. As generally observed on cuprates [28], iridates [23], and ruthenates [17,18], the t_{2g} and e_g states can be probed through oxygen hybridization on both the apical and planar oxygen sites, which have slightly different absorption resonance energies [28].

By varying light polarization and incident angle θ, matrix elements favor different p orbitals—see top panels of Fig. 1. Linear vertical light is, independent of incidence angle, mostly sensitive to the oxygen p_y orbitals. By contrast, linear-horizontal light predominantly probes p_x orbitals for $\theta = 0^\circ$ and p_z for $\theta \sim 90^\circ$. The degree of hybridization between the ruthenium (Ru^{4+}) $4d$ orbitals and the oxygen p_x, p_y, and p_z orbitals also enters into the absorption cross section. Therefore, varying incident angle θ and polarization on both planar and apical oxygen edges yields information about both ruthenium e_g and t_{2g} states.

The first two features in Figs. 1(a)–1(d)—appearing just below 530 eV—are the oxygen-K absorption resonances due

to Ru t_{2g} hybridization with apical and planar oxygen, respectively [17,18]. Features at higher energies are attributed to hybridization with e_g ($d_{3z^2-r^2}$ and $d_{x^2-y^2}$) Ru orbitals [17]. The $d_{3z^2-r^2}$ states are best probed through p_z hybridization on the apical oxygen site [see Fig. 2(a)]. Comparing t_{2g} (d_{xy},d_{xz},d_{yx}) and $d_{3z^2-r^2}$ apical absorption resonances suggests a splitting of approximately 2 eV in Ca_2RuO_4. In a similar fashion, $d_{x^2-y^2}$ states are best probed through the planar oxygen sites. There, the t_{2g} to $d_{x^2-y^2}$ splitting [Fig. 2(b)] is ~3–4 eV. Comparable energy scales were found in Sr_2RuO_4.

Next, we turn to the resonant inelastic x-ray spectra recorded on Ca_2RuO_4 and Sr_2RuO_4. In Fig. 2(c), the incident-photon-energy dependence of the RIXS spectra across apical and planar oxygen K resonances on Ca_2RuO_4 is shown for linear horizontal light polarization at incident angle $\theta = 75°$. Besides elastic scattering, three pronounced excitations are resolved at the planar oxygen edge. Those at ~2 and ~4 eV, correspond approximately to the t_{2g} to $d_{3z^2-r^2}$ and $d_{x^2-y^2}$ splittings and are hence assigned to be dd excitations. In the following, focus is on the low-energy excitations found at 0.3–0.5 eV for both Ca_2RuO_4 and Sr_2RuO_4(see Fig. 3). These excitations are nondispersive and reside at energies well above optical phonon branches. Furthermore, as Ca_2RuO_4 is an insulator, a plasmon scenario is very unlikely. These are also incompatible with a simple t_{2g} crystal field splitting, which is expected to be much smaller than 300 meV.

IV. INTERPRETATION

To gain further insight into the nature of this excitation, we start by discussing the t_{2g} states. Linear dichroism effects on x-ray absorption spectra yield information about the orbital hole occupation $n_3^{xz} = n_3^{yz}$ and n_3^{xy} [17,23]. For example, on the planar oxygen site, $p_{x/y} - d_{xy}$ and $p_z - d_{xz/yz}$ hybridizations are dominating, whereas $p_{x/y} - d_{xz/yz}$ is leading at the apical site. Using light polarization to emphasize the p_x or p_y channel, absorption is enhanced on the apical site if hole orbital occupation $n_3^{yz} = n_3^{xz}$ is high. Likewise, the planar absorption resonance will be enhanced for large d_{xy} occupation. As a result, apical and planar absorptions cannot both be strong at the same time.

The proportion between planar and apical XAS peak amplitudes is an experimental measure of the ratio $R_3 = n_3^{xy}/(n_3^{xz} + n_3^{yz})$ [17,23]. Judging from peak amplitudes [17],

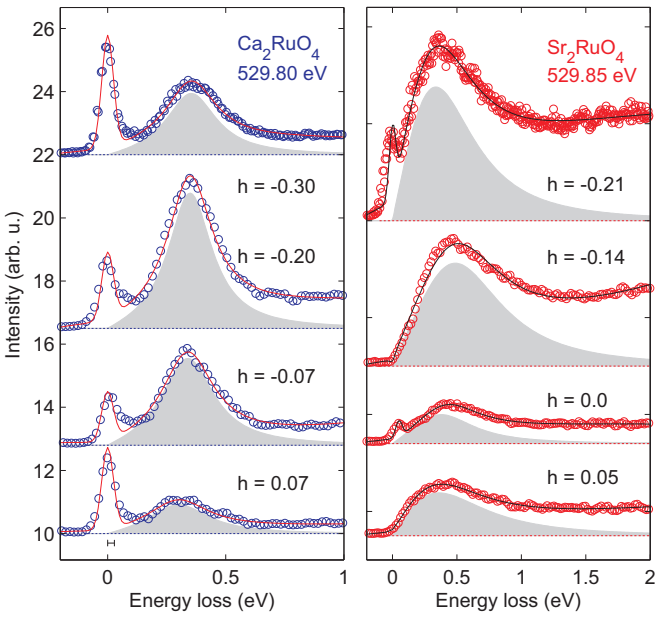

FIG. 3. (Color online) RIXS spectra for different momentum transfers $Q_{||} = (h,0)$ as indicated on Ca_2RuO_4 (left) and Sr_2RuO_4 (right), recorded using linear-horizontal light tuned to the planar oxygen K edge. For visibility, all spectra are given an individual vertical offset. Solid lines are fits to a Gaussian (approximately resolution limited elastic line), an antisymmetric Lorentzian (gray-shaded component), and a quadratic background.

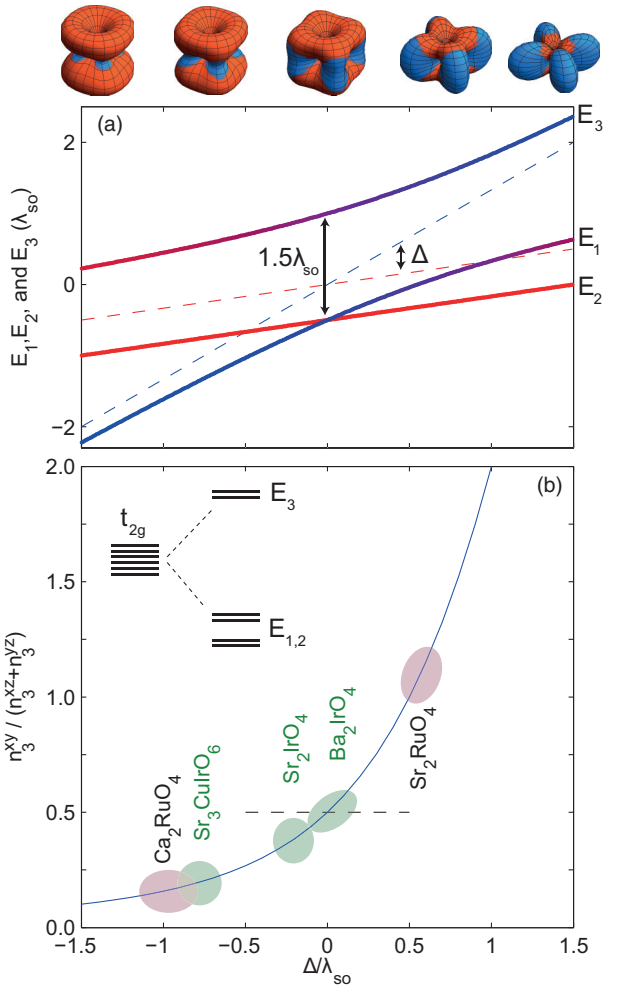

FIG. 4. (Color online) (a) Eigenenergies E_3, E_2, and E_1 of the Hamiltonian given in Eq. (1) versus Δ/λ_{so}, where Δ is the crystal field splitting of the t_{2g} states and λ_{so} is the spin-orbit-coupling strength. Dashed (solid) lines are the solutions in absence (presence) of spin-orbit interaction. Color indicates the orbital character with blue being d_{xy} and red being d_{yz} or d_{xz}. Top panels display the orbital topology of the E_3 eigenstate. (b) Ratio $n_3^{xy}/(n_3^{xz} + n_3^{xz})$ between orbital occupation of d_{xy} and d_{xz} versus Δ/λ_{so}. The solid line is the model expectation of the Hamiltonian given in Eq. (1). Values of Δ/λ_{so} for the iridate materials stem from Refs. [3,22,23,29]. The inset shows schematically how the t_{2g} states are split by spin-orbit interaction and crystal field.

$R_3 \sim 1.23(2)$ and $\sim 0.17(2)$, respectively in Sr_2RuO_4 and Ca_2RuO_4 [see Fig. 4(b)]. There is, however, a caveat related to the tetragonal distortion of the apical oxygen (6% and −2% in Sr_2RuO_4 and Ca_2RuO_4, respectively) leading to a slight under- and overestimation of $n_3^{xz/yz}$ [23]. Assuming (as done for iridate materials [23]) that the hybridization strength decays as $r^{-3.5}$ [30], where r is the Ru-O bond length, $n_3^{xz/yz}$ would be overestimated by ∼20% in Sr_2RuO_4 and underestimated by 5% in Ca_2RuO_4. Therefore, $1 < R_3 < 1.25$ for Sr_2RuO_4 and $0.15 < R_3 < 0.2$ for Ca_2RuO_4 (Fig. 4)—the latter being consistent with the conclusion of early XAS work at 90 K using circular polarized light [17].

V. MODEL

This mixing of $d_{xy}^{\pm}$, $d_{yz}^{\pm}$, and $d_{xz}^{\pm}$ orbitals, where ± refers to the electronic spin, can be explained by a non-negligible spin-orbit interaction λ_{so} [17,20,21,31,32]. Calculations including crystal field effects and spin-orbit interaction but neglecting the Hund's coupling [33] have described very successfully the band structure of Sr_2RuO_4 and Sr_2RhO_4 [20,21]. Following this spirit, the simplest Hamiltonian describing the t_{2g} states reads

$$H = \lambda_{so}\mathbf{L}\cdot\mathbf{S} + \frac{\Delta}{3}\langle L_z\rangle^2, \tag{1}$$

where $\mathbf{S}$ and $\mathbf{L}$ are the spin and orbital momentum operators and λ_{so} is the spin-orbit-coupling constant [22,23,34]. The intra-t_{2g} crystal field splitting Δ is defined so that $\Delta > 0$ lifts d_{xy} above d_{xz} and d_{yz}. Diagonalizing Eq. (1) in the ($d_{xy}^{\pm}$, $d_{yz}^{\pm}$, $d_{xz}^{\pm}$) subspace [22,34] (neglecting e_g states) yields the eigenstates $\psi_1^{\pm} = d_{xz}^{\mp} \pm i d_{yz}^{\mp} + \sqrt{n_1^{xy}} d_{xy}^{\pm}$, $\psi_2^{\pm} = d_{xz}^{\pm} \mp i d_{yz}^{\pm}$, and $\psi_3^{\pm} = d_{xz}^{\mp} \pm i d_{yz}^{\mp} + \sqrt{n_3^{xy}} d_{xy}^{\pm}$ with hole/electron occupancy:

$$n_3^{xy} = \frac{[2\delta - 1 + C]^2}{4} \quad \text{and} \quad n_1^{xy} = n_3^{xy} - 2C, \tag{2}$$

where $\delta = \Delta/\lambda_{so}$ and $C = \sqrt{9 + 4\delta(\delta - 1)}$ (see Fig. 4). The eigenenergies (E_3, E_2, and E_1) are split by

$$E_3 - E_1 = \frac{\lambda_{so} C}{2} \quad \text{and} \quad E_3 - E_2 = \frac{\lambda_{so}}{4}(C + 3 + 2\delta). \tag{3}$$

Notice that in the limit $\delta \to 0$ (the case of $\{Ba,Sr\}_2IrO_4$ [3,23,29]), $E_2 = E_1$ are degenerate [see Fig. 4(a)] and $E_3 - E_1 = 1.5\lambda_{so}$. In the opposite limit $\lambda_{so} \to 0$, $E_3 - E_1 = \Delta$. Within this simple model, our observables $R_3 = n_3^{xy}/(n_3^{xz} + n_3^{yz})$ and the RIXS excitation at ∼350 meV can be explained using the two adjustable parameters Δ and λ_{so}.

For example, for Sr_2RuO_4 where $R_3 \approx 1.2(2)$, we find $\Delta/\lambda_{so} \sim 0.55(5)$ (see Fig. 4). This implies that $E_3 - E_1 = 1.4\lambda_{so}$ and $E_3 - E_2 = 2.1\lambda_{so}$. Assuming that the peak feature at ∼350 meV [Fig. 3(a)] results from the average of two broad excitations ($E_3 - E_2$ and $E_3 - E_1$) leads us to $\lambda_{so} \sim 200$ meV and hence $\Delta \sim 100$ meV. This value of λ_{so} is comparable to the theoretical expectation for Ru [20,35] and what has been extracted from spin-resolved angle-resolved photoemission spectroscopy [20]. Notice that the $E_2 - E_1 \sim \Delta/2 \approx 50$ meV splitting—possibly accessible through indirect RIXS processes—is expected near the elastic line but not resolved in this experiment.

As $R_3 \sim 1/6$ for Ca_2RuO_4, it implies that $\delta \sim -1$ and hence $E_3 - E_1 = 2.1\lambda_{so}$ and $E_3 - E_2 = 1.3\lambda_{so}$. The RIXS spectra, shown in Fig. 3(a), exhibit a pronounced excitation at ∼350 meV. If this is a result of an average of two excitations, once again $\lambda_{so} \sim 200$ meV is found. Thus, by including a spin-orbit coupling of 200 meV, a consistent description of the orbital hole occupation extracted from XAS and the excitations of the RIXS spectra on both Sr_2RuO_4 and Ca_2RuO_4 is obtained.

VI. DISCUSSION

Implications of spin-orbit coupling λ in 4d-transition oxide materials have already been evaluated in a number of papers [10,14,21,31,32,35,36]. The magnon band-width in Ca RuO is, for example, predicted [10] to be controlled by $\sim 3\lambda/4$. Neutron experiments should be performed to test this prediction. Magnetic moments are also influenced but not uniquely defined by Δ/λ [10]. As the experiments on Ca_2RuO_4 suggest that $\psi_3^{\pm}$ is dominated by d_{xz}/d_{yz} orbitals, it is possible to approximate $\psi_3^{\pm} \approx d_{xz}^{\mp} \pm i d_{yz}^{\mp}$. Then, both $\psi_2^{\pm}$ and $\psi_3^{\pm}$ are more elegantly expressed in spherical harmonic notation: $\psi_2^{\pm} = |\ell_z = \pm 1, s_z = \mp 1/2\rangle = \chi^{\pm 1/2}$ and $\psi_3^{\pm} = |\ell_z = \pm 1, s_z = \pm 1/2\rangle = \chi^{\pm 3/2}$. In this simplistic limit, the role of spin-orbit interaction is to split the fourfold degeneracy of $d_{xz}^{\pm}$ and $d_{yz}^{\pm}$ into twofold degenerated $\chi^{\pm 3/2}$ and $\chi^{\pm 1/2}$ states (see Fig. 4). It has been argued that even modest Coulomb interaction U is sufficient to split these $\chi^{\pm 3/2}$ and $\chi^{\pm 1/2}$ states and hence drive the Mott insulating transition [31,32]. Therefore, as in layered iridates, a combination of spin-orbit interaction and electron correlations may be sufficient to drive the Mott insulating ground state.

Another interesting question is how spin-orbit interaction impacts the superconducting ground state in Sr_2RuO_4 [37]. It has been suggested theoretically that ferromagnetic interactions would result in a chiral p-wave superconducting state [13] driven by the d_{xy}-dominated γ band. By contrast, if superconductivity is driven by the d_{xz}/d_{yz}-dominated α and β bands [12], then spin-orbit coupling lifts the ground state degeneracy in favor of a helical p-wave symmetry [14]. These considerations were, however, based on the assumption that spin-orbit interaction is weak compared to the Fermi energy E_F [14]. It is hence useful to compare the energy scales of superconductivity, spin-orbit coupling, and the Fermi energy. As $T_c = 1.5$ K, the superconducting gap amplitude is expected in the ∼1 meV range [38]. The Fermi energy $E_F = [\hbar/(4\pi k_B)](A_k/m^*)$ [39] can be estimated from the Fermi surface area A_k and the quasiparticle mass m^*. For the γ band, quantum oscillation experiments [11] yield oscillation frequency $\hbar A_k/2e\pi = 18$ kT and $m^* = 16m_e$, where m_e is the free electron mass. These values imply that $E_F \sim 150$ meV, and as expected $k_B T_c/E_F \ll 1$. Similar values of E_F are found for the α and β bands. Strong electron correlations therefore drive even the γ electrons into the regime $\lambda_{so} \sim E_F$, where spin S_z and orbital L_z are no longer good quantum numbers. Cooper pairs in Sr_2RuO_4 therefore have to be composed of electronic pseudospins. If realized, the same would likely be true for superconductivity in layered iridates.

VII. CONCLUSIONS AND OUTLOOK

In summary, we have performed a combined light absorption and oxygen K-edge resonant inelastic x-ray spectroscopy study of the ruthenates $(Ca,Sr)_2RuO_4$. Special attention was given to the Ru t_{2g} states, probed through their hybridization with oxygen p orbitals. Both the oxygen K-edge RIXS and absorption spectra find a consistent description within a simple model that includes crystal field splitting and spin-orbit coupling $\lambda_{so} \approx 200$ meV. In this picture, the main new observation—RIXS excitations at ~350 meV—is interpreted as holes moving across spin-orbit split t_{2g} states.

ACKNOWLEDGMENTS

We thank M. Sigrist and V. M. Katukuri for enlightening discussions. This research is funded by the Swiss National Science Foundation and its Sinergia network Mott Physics Beyond the Heisenberg (MPBH) model. Experiments have been performed at the ADRESS beamline of the Swiss Light Source at Paul Scherrer Institut. J.P. and T.S. acknowledge financial support through the Dysenos AG by Kabelwerke Brugg AG Holding, Fachhochschule Nordwestschweiz, and the Paul Scherrer Institut.

[1] M. Z. Hasan and C. L. Kane, Rev. Mod. Phys. **82**, 3045 (2010).
[2] W. Witczak-Krempa, G. Chen, Y. B. Kim, and L. Balents, Ann. Rev. Condens. Matter Phys. **5**, 57 (2014).
[3] B. J. Kim, H. Jin, S. J. Moon, J.-Y. Kim, B.-G. Park, C. S. Leem, J. Yu, T. W. Noh, C. Kim, S.-J. Oh, J.-H. Park, V. Durairaj, G. Cao, and E. Rotenberg, Phys. Rev. Lett. **101**, 076402 (2008).
[4] F. Wang and T. Senthil, Phys. Rev. Lett. **106**, 136402 (2011).
[5] E. Gorelov, M. Karolak, T. O. Wehling, F. Lechermann, A. I. Lichtenstein, and E. Pavarini, Phys. Rev. Lett. **104**, 226401 (2010).
[6] T. Hotta and E. Dagotto, Phys. Rev. Lett. **88**, 017201 (2001).
[7] J. H. Jung, Z. Fang, J. P. He, Y. Kaneko, Y. Okimoto, and Y. Tokura, Phys. Rev. Lett. **91**, 056403 (2003).
[8] J. S. Lee, Y. S. Lee, T. W. Noh, S.-J. Oh, J. Yu, S. Nakatsuji, H. Fukazawa, and Y. Maeno, Phys. Rev. Lett. **89**, 257402 (2002).
[9] I. Zegkinoglou, J. Strempfer, C. S. Nelson, J. P. Hill, J. Chakhalian, C. Bernhard, J. C. Lang, G. Srajer, H. Fukazawa, S. Nakatsuji, Y. Maeno, and B. Keimer, Phys. Rev. Lett. **95**, 136401 (2005).
[10] A. Akbari and G. Khaliullin, Phys. Rev. B **90**, 035137 (2014); G. Khaliullin, Phys. Rev. Lett. **111**, 197201 (2013).
[11] A. P. Mackenzie and Y. Maeno, Rev. Mod. Phys. **75**, 657 (2003).
[12] S. Raghu, S. A. Kivelson, and D. J. Scalapino, Phys. Rev. B **81**, 224505 (2010).
[13] T. M. Rice and M. Sigrists, J. Phys: Condens. Matter **7**, L643 (1995).
[14] Y. Yanase, S. Takamatsu, and M. Udagawa, J. Phys. Soc. Jpn. **83**, 061019 (2014).
[15] I. I. Mazin and D. J. Singh, Phys. Rev. Lett. **79**, 733 (1997).
[16] I. I. Mazin and D. J. Singh, Phys. Rev. Lett. **82**, 4324 (1999).
[17] T. Mizokawa, L. H. Tjeng, G. A. Sawatzky, G. Ghiringhelli, O. Tjernberg, N. B. Brookes, H. Fukazawa, S. Nakatsuji, and Y. Maeno, Phys. Rev. Lett. **87**, 077202 (2001).
[18] M. Malvestuto, E. Carleschi, R. Fittipaldi, E. Gorelov, E. Pavarini, M. Cuoco, Y. Maeno, F. Parmigiani, and A. Vecchione, Phys. Rev. B **83**, 165121 (2011).
[19] M. Malvestuto, V. Capogrosso, E. Carleschi, L. Galli, E. Gorelov, E. Pavarini, R. Fittipaldi, F. Forte, M. Cuoco, A. Vecchione, and F. Parmigiani, Phys. Rev. B **88**, 195143 (2013).
[20] C. N. Veenstra, Z.-H. Zhu, M. Raichle, B. M. Ludbrook, A. Nicolaou, B. Slomski, G. Landolt, S. Kittaka, Y. Maeno, J. H. Dil, I. S. Elfimov, M. W. Haverkort, and A. Damascelli, Phys. Rev. Lett. **112**, 127002 (2014).
[21] M. W. Haverkort, I. S. Elfimov, L. H. Tjeng, G. A. Sawatzky, and A. Damascelli, Phys. Rev. Lett. **101**, 026406 (2008).
[22] X. Liu, V. M. Katukuri, L. Hozoi, W.-G. Yin, M. P. M. Dean, M. H. Upton, J. Kim, D. Casa, A. Said, T. Gog, T. F. Qi, G. Cao, A. M. Tsvelik, J. van den Brink, and J. P. Hill, Phys. Rev. Lett. **109**, 157401 (2012).
[23] M. Moretti Sala, M. Rossi, S. Boseggia, J. Akimitsu, N. B. Brookes, M. Isobe, M. Minola, H. Okabe, H. M. Rønnow, L. Simonelli, D. F. McMorrow, and G. Monaco, Phys. Rev. B **89**, 121101 (2014).
[24] K. Deguchi, M. A. Tanatar, Z. Mao, T. Ishiguro, and Y. Maeno, J. Phys. Soc. Jpn. **71**, 2839 (2002).
[25] S. Nakatsuji and Y. Maeno, J. Solid State Chem. **156**, 26 (2001).
[26] V. Strocov, T. Schmitt, U. Flechsig, T. Schmidt, A. Imhof, Q. Chen, J. Raabe, R. Betemps, D. Zimoch, J. Krempasky, X. Wang, M. Grioni, A. Piazzalunga, and L. Patthey, J. Synchrotron Radiat. **17**, 631 (2010).
[27] G. Ghiringhelli, A. Piazzalunga, C. Dallera, G. Trezzi, L. Braicovich, T. Schmitt, V. N. Strocov, R. Betemps, L. Patthey, X. Wang, and M. Grioni, Rev. Sci. Instrum. **77**, 113108 (2006).
[28] C. T. Chen, F. Sette, Y. Ma, M. S. Hybertsen, E. B. Stechel, W. M. C. Foulkes, M. Schluter, S.-W. Cheong, A. S. Cooper, L. W. Rupp, B. Batlogg, Y. L. Soo, Z. H. Ming, A. Krol, and Y. H. Kao, Phys. Rev. Lett. **66**, 104 (1991).
[29] J. Kim, M. Daghofer, A. H. Said, T. Gog, J. van den Brink, G. Khaliullin, and B. J. Kim, Nat. Commun. **5**, 4453 (2014).
[30] W. A. Harrison, *Electronic Structure and the Properties of Solids: The Physics of the Chemical Bond* (W. H. Freeman and Company, New York, 1980).
[31] G.-Q. Liu, Phys. Rev. B **84**, 235136 (2011).
[32] G.-Q. Liu, Phys. Rev. B **88**, 104428 (2013).
[33] A. Georges, L. de' Medici, and J. Mravlje, Ann. Rev. Condens. Matter Phys. **4**, 137 (2013).
[34] M. Moretti Sala, S. Boseggia, D. F. McMorrow, and G. Monaco, Phys. Rev. Lett. **112**, 026403 (2014).
[35] H. Kontani, T. Tanaka, D. S. Hirashima, K. Yamada, and J. Inoue, Phys. Rev. Lett. **100**, 096601 (2008).
[36] H. Iwasawa, Y. Yoshida, I. Hase, S. Koikegami, H. Hayashi, J. Jiang, K. Shimada, H. Namatame, M. Taniguchi, and Y. Aiura, Phys. Rev. Lett. **105**, 226406 (2010).
[37] M. Tsuchiizu *et al.*, Phys. Rev. B **91**, 155103 (2015).
[38] I. A. Firmo, S. Lederer, C. Lupien, A. P. Mackenzie, J. C. Davis, and S. A. Kivelson, Phys. Rev. B **88**, 134521 (2013).
[39] J. Chang, R. Daou, C. Proust, D. LeBoeuf, N. Doiron-Leyraud, F. Laliberté, B. Pingault, B. J. Ramshaw, R. Liang, D. A. Bonn, W. N. Hardy, H. Takagi, A. B. Antunes, I. Sheikin, K. Behnia, and L. Taillefer, Phys. Rev. Lett. **104**, 057005 (2010).